ELSEVIER

Journal of Fluorine Chemistry 79 (1996) 59–69

JOURNAL OF FLUORINE CHEMISTRY

Diblock and triblock semifluorinated n-alkanes: preparations, structural aspects and applications

M. Napoli

Institute of Industrial Chemistry, University of Padua, via Marzolo 9, 35131 Padua, Italy

Received 18 December 1995; accepted 20 February 1996

Abstract

The results of several recent studies on a new family of compounds consisting of linear semifluorinated n-alkanes with a diblock or triblock structure are reviewed. Special emphasis is laid on their morphology and structural characteristics in the crystalline state and on their phase transitions either in the solid or in the crystalline liquid state, surface activity in organic solvents and the formation of a gel-like phase. Recently proposed applications for these compounds are also reported.

Keywords: Diblock semifluorinated alkanes; Triblock semifluorinated alkanes; (Perfluoroalkyl) alkanes; Amphiphilic molecules; Raman spectroscopy; SAX scattering; DSC thermal analysis

1. Introduction

Diblock and triblock semifluorinated n-alkanes are a particular class of fluorinated compounds which in recent years have been the subject of numerous studies, especially regarding their structure and properties in the solid, solution and melt state. These compounds have a characteristic linear molecular structure consisting of a hydrocarbon segment $H(CH_2)_m-$ linked to a fluorocarbon segment $-(CF_2)_nF$ for diblock compounds, and of a hydrocarbon segment $-(CH_2)_m-$ symmetrically linked to two fluorocarbon segments $F(CF_2)_n-$ for triblock compounds; m and n are generally even numbers ranging from 2 to 20 (for m) or to 12 (for n). The general molecular structures are therefore $F(CF_2)_n(CH_2)_mH$ and $F(CF_2)_n(CH_2)_m(CF_2)_nF$, respectively.

These molecules are of particular interest because they can be considered in essence as low molecular weight block copolymers of normal fluorocarbons and hydrocarbons. Their structural characteristics and behaviour can give useful information for predicting the corresponding properties of their fluorinated macromolecular chain analogues, such as $-[(CF_2)_x-(CH_2)_y-]_n-$ or $-(CF_2-CH_2)_n-$, or $-(CF_2CF_2-CH_2CH_2)_n-$. Spectrometric measurements give important information on the molecular conformation and crystalline structure of these compounds, and solid–solid phase transitions have been revealed by thermal analysis.

These semifluorinated n-alkanes show a particular behaviour in solutions of organic solvents with the formation of reversed micelles and, in consequence of cooling, of a phase exhibiting gel-like characteristics; due to their amphiphilic structure, which arises from the incompatibility of the constituent segments, they have been defined as a new class of surfactant. In spite of the $-CF_2-CH_2-$ linkage which inserts an element of discontinuity into the structure, these compounds also show a high chemical and biological stability which allows their utilization in the biomedical field. This application is mainly related to their interfacial activity in the microemulsions used as O_2-transporting fluids for the same reason, diblock semifluorinated n-alkanes have been recently tried as additives in the ski-wax preparation.

The purpose of this paper is therefore to review what has so far been reported with regard to the synthesis, structural characteristics, behaviour in solution and applications for these interesting fluorinated compounds.

2. Preparation

The preparation of these semifluorinated alkanes is generally accomplished in two steps consisting of (1) the addition of a perfluoroalkyl iodide, $F(CF_2)_nI$, to a linear 1-alkene and (2) the subsequent reduction of the iodine-containing adduct so formed. The procedure is essentially the same for preparing either diblock or triblock semifluorinated alkanes (hereafter referred to as F_nH_m and $F_nH_mF_n$, respectively), but some particular aspects are pointed out in the preparation of $F_nH_mF_n$.

PII S0022-1139(96)03439-2

2.1. Preparation of F_nH_m compounds

The first stage consists of the extensively investigated addition of perfluoroalkyl iodides to unsaturated systems, in this case 1-alkenes, to give the corresponding iodo adduct:

$$F(CF_2)_nI + CH_2=CH-(CH_2)_{m-2}H \longrightarrow$$
$$F(CF_2)_n-CH_2I-(CH_2)_{m-2}H$$

Further addition of the iodine-containing adduct to the 1-alkene to give $F(CF_2)_nCH_2CH[(CH_2)_{m-2}H]CH_2CHI(CH_2)_{m-2}H$ can occur, depending mainly on the molar ratio of the reagents.

Induction of the reaction can be performed thermally at 200–220°C [1–4], electrochemically [5], by the use of ultraviolet light [6,7] or X-Rays [8], or in a redox system [9,10]: in these cases, however, complex mixtures are obtained from which, especially with long-chain olefins, the desired product can only be isolated with difficulty, frequently in an impure condition. Much better results are obtained using a metal [11,12] or a free-radical generating initiator: hydrogen peroxide [13], α,α'-azobis(dimethylvaleronitrile) [14–16], α,α'-azobis(cyclohexanecarbonitrile) [17], di-t-butyl peroxide [8,18,19], benzoyl peroxide [7,17], and especially α,α'-azobis(isobutyronitrile) [8,15,17,20,21] have often been used for this purpose. Equimolecular amounts of the reagents can be used, but an excess of perfluoroalkyl iodide, which is readily recovered, allows the reduction of the consecutive addition of the iodo adduct to the alkene. Other operational conditions (temperature, reaction time) depend on the reagents and the amount of initiator used [21].

The second step consists of the reductive dehalogenation of the iodo adduct:

$$F(CF_2)_n-CH_2CHI-(CH_2)_{m-2}H \longrightarrow F(CF_2)_n(CH_2)_mH$$

which can be accomplished by treatment with zinc powder in acetic acid [22] or in either gaseous [17,23,24] or aqueous [17,21,25] HCl in ethanol or another solvent (such as methanol, propanol, acetone), or with lithium aluminium hydride in anhydrous diethyl ether [15,21], or with tributyltin hydride [2,26].

In an alternative method proposed for preparing the diblock semifluorinated n-alkanes, the reaction of a perfluoroalkyl iodide with a 1-alkene can be performed in the presence of activated copper bronze using DMSO as solvent [27]. In this manner a mixture of the semifluorinated n-alkane with some of the corresponding olefin $F(CF_2)_n$–CH=CH–$(CH_2)_{m-2}H$ was obtained. Subsequent reduction of this mixture with hydrogen and palladium on charcoal using ethanol as solvent afforded the semifluorinated n-alkane as the sole isolable product.

Unsaturated diblocks $F(CF_2)_nCH_2$ CH=CH $(CH_2)_{m-3}H$, from which the corresponding semifluorinated n-alkane $F(CF_2)_n(CH_2)_mH$ can be easily obtained by hydrogenation of the double bond, have also been prepared by Wittig reaction in phase-transfer catalysis starting from phosphonium iodides $Ph_3P^+CH_2CH_2(CF_2)_nCF_3\ I^-$ and aldehydes $H(CH_2)_{m-3}CHo$ [28,29].

Another reported method of synthesis [25] consists in a three-step reaction starting from perfluorocarboxylic esters and alkylmagnesium bromides:

$$F(CF_2)_nCOOMe + H(CH_{2m-1}MgBr \longrightarrow$$
$$F(CF_2)_nCH(OH)(CH_2)_{m-1}H$$

Subsequent treatment of the alcohol with P_2O_5 at 200°C gives the olefin $F(CF_2)_nCH=CH(CH_2)_{m-2}H$, from which the corresponding diblock $F(CF_2)_n(CH_2)_mH$ is obtained by catalyzed (Rh/C) hydrogenation under pressure (100 atm) and at ambient temperature (25°C).

2.2. Preparation of $F_nH_mF_n$ compounds

The preparation of triblock semifluorinated n-alkanes should be carried out under conditions essentially identical with those used for diblock compounds [30]. However, with long perfluoroalkyl iodides ($m>10$) and diolefins ($n>20$) the preparation of triblock compounds requires some modifications.

In experiments performed with perfluorododecyl iodide and 1,21-docosadiene [24], the initial reaction between perfluoroalkyl iodide and the dialkene was not significantly modified except that routine analysis of the progress of the reaction by gas chromatography was not possible. In contrast, the dehalogenation reaction was particularly troublesome because the intermediate was not soluble and did not melt in boiling ethanol; the use of higher boiling alcohols together with a co-solvent such as n-octane was necessary. Also, it was difficult to monitor the progress of the dehalogenation reaction by gas chromatography, and large excesses of hydrogen chloride and zinc had to be used to ensure complete reduction.

Other problems were found when di-olefins having four or seven carbon atoms were used in this reaction: with 1,3-butadiene the reaction led to an unstable product [24] and with 1,6-heptadiene cyclic compounds were predominantly obtained [16,30].

A recent alternative method [31] achieves the preparation of triblock semifluorinated n-alkanes by treatment of $F(CF_2)_n(CH_2)_mI$ with Mg in an aprotic anhydrous solvent at 40–140°C under normal or elevated pressure; in this manner $F(CF_2)_n(CH_2)_{2m}(CF_2)_nF$ compounds can be obtained.

Triblock $H(CH_2)_m(CF_2)_n(CH_2)_mH$ compounds have been starting from perfluorodicarboxylic acids and alkylmagnesium bromides [25]:

$$HOCO(CF_2)_{n-2}COOH + H(CH_2)_mMgI \longrightarrow$$
$$H(CH_2)_mCO(CF_2)_{n-2}CO(CH_2)_mH$$

Subsequent treatment with HF and SF_4 of the diketone so formed afforded the corresponding triblock semifluorinated n-alkane.

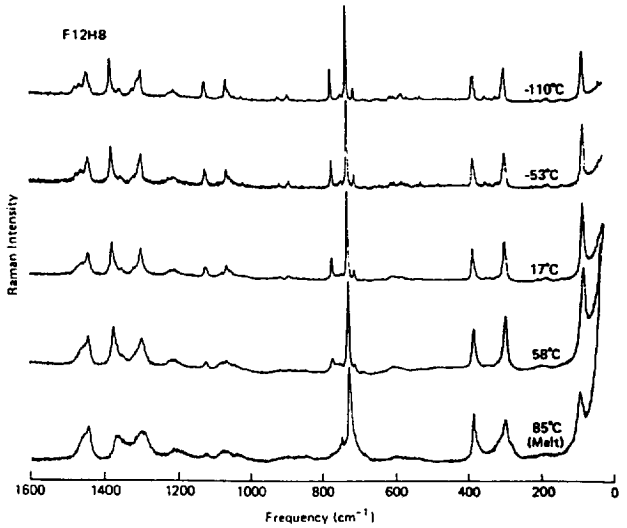

Fig. 1. Raman spectra of $F_{12}H_8$ recorded at various temperatures below and above the solid–solid phase transition (taken from Ref. [32]).

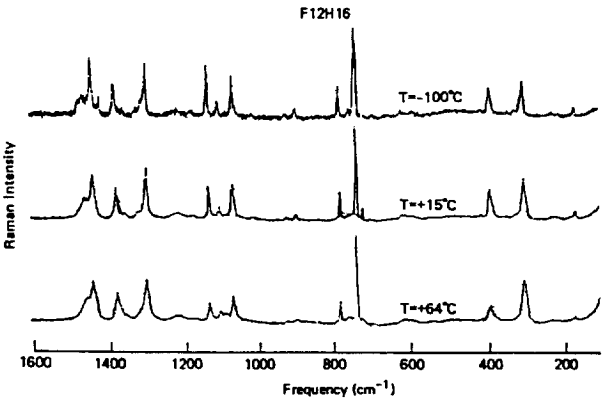

Fig. 2. Raman spectra of $F_{12}H_{16}$ recorded at various temperatures (taken from Ref. [32]).

3. Structural aspects

3.1. Molecular conformations in the solid state

Measurements of the Raman spectra as a function of temperature of diblock semifluorinated compounds of the $F_{12}H_m$ series [32] give important details on the molecular conformations of these compounds in the solid state. In the spectrum of $F_{12}H_8$, recorded at 17°C and reported in Fig. 1 as a typical example of the spectra observed for these compounds, the main characteristic is the small overlap between bands relative to either the hydrogenated or fluorinated segments of the molecule. In particular, the sharp bands in the 200–800 cm^{-1} region and those at 1215, 1296 and 1385 cm^{-1} are assigned to vibrations of the fluorocarbon segment (helical conformation), while the remaining medium bands are reported as being attributable to vibrations of the hydrogenated segment (planar zig-zag conformation). The very intense band observed below 200 cm^{-1} is assigned to the Raman-active longitudinal acoustical mode (LAM), i.e. to a composite vibration involving an accordion-like motion of the entire molecule without decoupling at the junction of the planar zig-zag and the helical segments. Thus, a change in its frequency can denote a change in the molecular length due to temperature-induced alterations in the conformation of either the helical fluorinated or the planar hydrogenated segment.

An increase in temperature above the solid–solid phase transition leads to very little change in the Raman spectrum (see the shape recorded at 58°C in Fig. 1). In particular, only a small decrease in intensity can be observed for the LAM, which maintains its frequency position however. All this suggests that the molecule also remains fully extended above the solid–solid transition and that only a change in the lattice packing, but not in the conformation, maybe associated with the transition itself. This is confirmed by the disappearance in the melt phase of the 1060 and 1130 cm^{-1} bands associated with the random conformation assumed by the hydrogenated segment (see the shape recorded at 85°C in Fig. 1) and still present at 58°C. The concomitant shift of the LAM vibration to higher frequency, which is observed in the same spectrum, also confirms this disorder, attributable to the presence of an ordered segment (fluorinated) linked to a disordered segment (hydrogenated) and leading to a decrease in the effective chain length.

Semifluorinated compounds having the hydrogenated segment longer than the fluorinated one show a different spectral behaviour as the temperature changes. These compounds do not show a solid–solid phase transition above the ambient temperature and the shape of their Raman spectra in the methylene bending region varies with temperature. Thus, in the 1400–1500 cm^{-1} region of the Raman spectrum recorded for $F_{12}H_{16}$ at 15°C (Fig. 2), two overlapping bands can be seen showing a different profile from that reported in Fig. 1 for $F_{12}H_8$ in the same region at 17°C. Instead, this latter is very similar to that reported in Fig. 2 for $F_{12}H_{16}$ at higher temperature (64°C). That suggests a different intermolecular arrangement of the hydrogenated segment in these two compounds; in particular, for $F_{12}H_{16}$ it suggests a closer packing of the chains at room temperature.

In the last analysis, Raman measurements indicate that the hydrogenated sequences in diblock semifluorinated n-alkanes do not assume a close packing in the lattice as in the case of polyethylene, but instead exhibit considerable motional freedom.

Triblock semifluorinated n-alkanes show a different band profile in the low-frequency region (30–330 cm^{-1}) of their Raman spectram, bolt at ambient temperature and in the melt state, as shown in Fig. 3 for $F_{12}H_8F_{12}$ [24]. At room temperature, three bands of medium intensity can be observed; the most intense (at 40 cm^{-1}) and the weakest (at 112 cm^{-1}) bands are assigned to the Raman-active LAM-1 and LAM-3 modes respectively, while the medium band at 295 cm^{-1} is assigned to a CF_2 bending vibration in the ordered fluorinated sequences. When the compound is heated above its melting point, both LAM-1 and LAM-3 bands disappear and are replaced by a broad band at 95 cm^{-1}. Similar results are

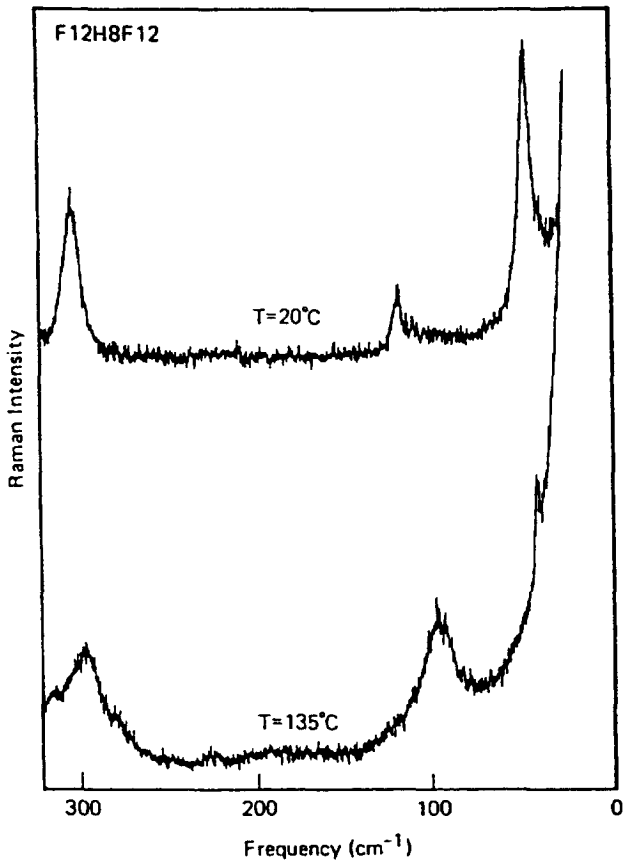

Fig. 3. Low-frequency (30–330 cm^{-1}) Raman spectra of $F_{12}H_8F_{12}$ recorded at ambient temperature and in the melt state (taken from Ref. [24]).

reported for other compounds in the series $F_{12}H_mF_{12}$ [24], confirming that, even if the LAM-1 and LAM-3 bands in the solid phase are at different frequencies depending on the examined triblock compound, the single broad band in the melt is always present in the 94 cm^{-1} region.

This behaviour can be explained by considering that in the solid phase the observed LAM-1 and LAM-3 bands maybe attributed to the longitudinal oscillations of the fully extended molecule; according to the inverse frequency/chain-length relationship generally observed for an LAM, a decrease in the LAM-1 and LAM-3 frequencies is observed when the molecule length increases (larger values of m). When the triblock compound melts, the central hydrogenated segment disorders, due to the disappearance of the intermolecular interactions that depend on the planar zig-zag conformation in the solid state. Instead the fluorinated segments retain their rod-like shape, since their helical conformation is stabilized by intramolecular steric effects; thus their LAM-1 frequency is not affected. In the last analysis, in the solid state the molecule is fully extended, while in the melt the intermediate hydrogenated segment becomes randomly disordered. The LAM-1 band observed in the melt thus results from the longitudinal oscillations of only the fluorinated segments.

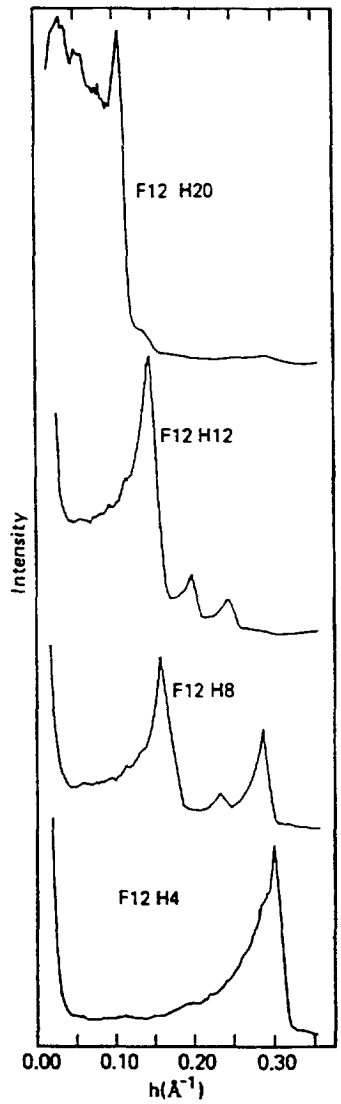

Fig. 4. SAXS profiles for some $F_{12}H_m$ compounds at the crystalline state (taken from Ref. [23]).

3.2. Molecular packing in the crystals

Further information concerning the organization of chains in the crystalline state of semifluorinated n-alkanes was obtained by X-ray diffraction measurements performed with some compounds of the series $F_{12}H_m$ [23]. In particular, the small-angle X-ray scattering (SAXS) technique was used; since hydrogen and fluorine have different electron densities, this provides a means of evaluating the electron density profile of the crystal as well as the manner in which crystals stack with respect to one another.

Fig. 4 shows the SAXS profiles obtained with the indicated $F_{12}H_m$ compounds. As can be seen, the general shape depends on the relative length of the hydrogenated and the fluorinated segments. Thus, for $m = 2$, 4 and 6, the SAXS consists of one sharp reflection which is characteristic of a single-crystal packing. When the hydrogenated segment increases in length, i.e., for $m = 8$, 10 and 12, three or four maxima can be

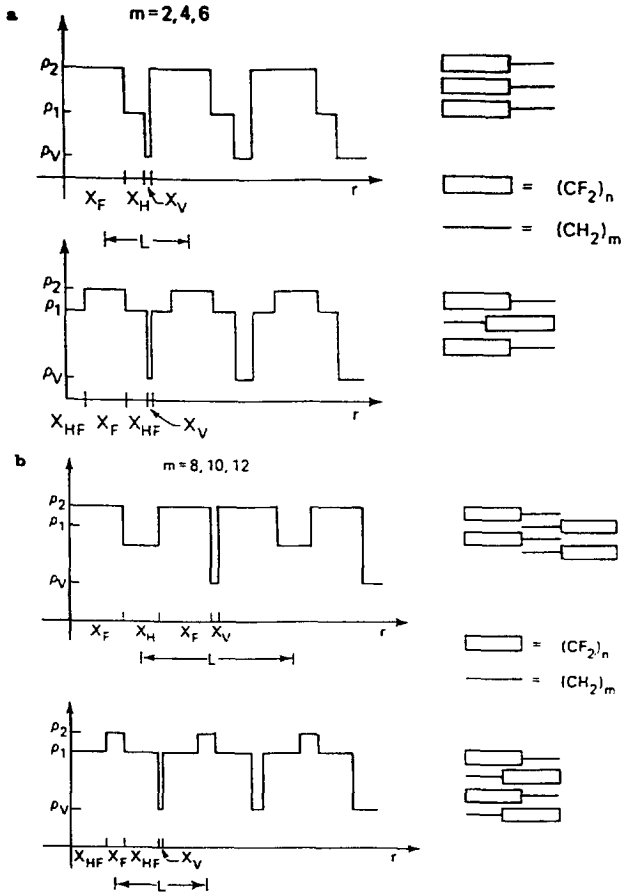

Fig. 5. Models for electron density profiles of $F_{12}H_m$; (a) $m=2$, 4 and 6; (b) $m=8$, 10 and 12 (taken from Ref. [23]).

observed; as these are related to first-order or second-order reflections, the co-existence of two different crystal packings can be suggested for these compounds at room temperature. For longer hydrogenated segments, i.e., for $m>14$, a single sharp reflection can be seen, together with a diffuse maximum at smaller scattering vectors. The former can be attributed to scattering arising from a bilayered structure whose existence provides a likely explanation for the rigidity of the helicoidal fluorinated segment.

A model for the electron density profiles which agrees with these experimental observations is reported in Fig. 5, where the electron density is reported as a function of distance r. The length of the hydrogenated and fluorinated portions of the crystal are represented as X_H and X_F, respectively; X_{HF} denotes a mixed section of the crystal, whereas V denotes the void existing between each crystal in the crystal stack. For $m=2$, 4 and 6, two different molecular packings can be suggested in order to describe the observed SAXS profiles [Fig. 5(a)]. In the first (*parallel* packing) the fluorinated and hydrogenated segments are next to one another, whereas in the second (*antiparallel* packing) the molecules are arranged so as to maximize the number of fluorine–hydrogen contacts. An *anti-parallel* packing can also be shown for $m=8$, 10 and 12 [Fig. 5(b)], in addition to a second *bilayered* packing where the hydrogenated segments are overlapped and interleaved between two layers of fluorinated segments packed adjacently. In particular, it should also be noted that these two structures can be interchanged by sliding the molecules along their axes. For $m>12$, the single sharp maximum observed could be related to the *bilayered* structure; no evidence was found in this case for the *antiparallel* packing.

The rate at which the crystal spacing increases as the hydrogenated sequence is lengthened defines how these molecular packing are arranged inside the crystal. For $m=2$, 4 and 6 the spacings are shorter than the molecular length and increase by less than 1.25 Å (i.e. the length assumed for a CH_2 segment [33]) for each additional CH_2 [23]; this suggests that the molecular chains are tilted with respect to the crystal surface. This tilt angle depends on the length of the hydrocarbon segment and values of 0°, 16.6° and 26.2° were determined for $m=2$, 4 and 6, respectively [30]. For $m=8$, 10, 12 and 14 the spacings are larger than the lengths of the individual molecules, and can be described only by a bilayered structure with overlapping of the hydrocarbon sequences. For $m>14$, a different, but not as yet precisely detailed, structure is evident.

As the temperature is increased above the transition value, a translation of the molecules occurs along their axes producing structural changes in the molecular packing [32]. In Fig. 6, the structural changes are represented by a model for the $F_{12}H_m$ compounds with $m\leq 6$, either for the *parallel* (structure A) or the *antiparallel* (structure B) tilted packing, below (on the left) and above (on the right) the transition temperature; the fluorinated and hydrogenated segments are represented by rectangles and solid lines, respectively. The same situation is represented in Fig. 7 for the $F_{12}H_m$ com-

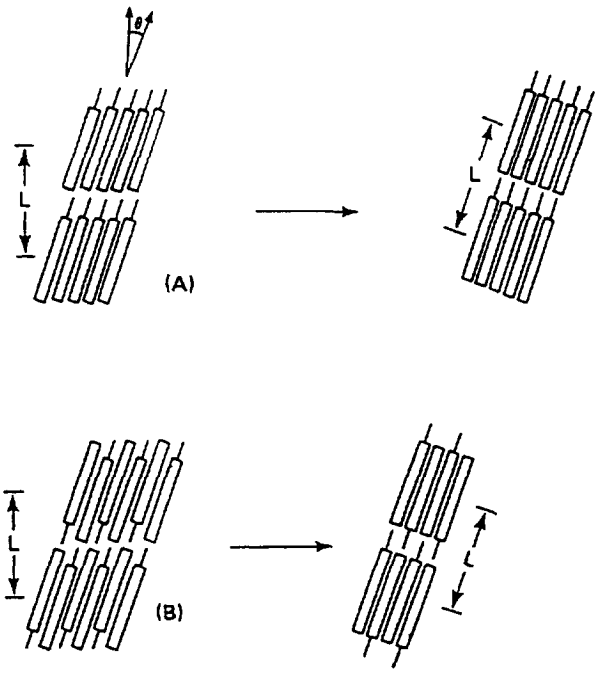

Fig. 6. Model for the molecular packing of $F_{12}H_m$ compounds with $m=2$, 4 and 6 (taken from Ref. [32]).

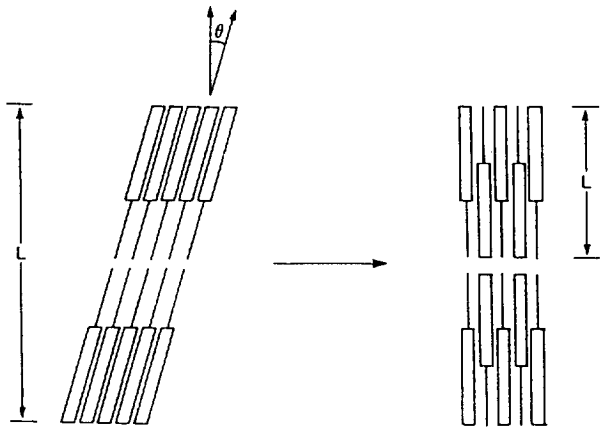

Fig. 7. Model for the molecular packing of $F_{12}H_m$ compounds with $m=8$, 10, 12 and 14 (taken from Ref. [32]).

pounds having $m>6$, for which a bilayered structure is suggested for the crystalline state.

More recently [34], a different model has been proposed with regard to the morphological structure of diblock semifluorinated n-alkanes in the crystalline state. Thus transmission electron microscopic observations on a freeze-fractured $F(CF_2)_{12}$ $(CH_2)_{20}H$ surface of a melt-crystallized sample exhibited stripes which exhibited a dominant periodical distance of 24 nm. Such a distance is not assigned to a lamellar structure, but to layers of cylinders having an uniform diameter of 24 nm. Assuming that the fully extended molecule has a length of ca. 4 nm, each cylinder should consist of three concentric layers; in this manner cylindrical crystallites are formed which have a morphological analogy with some silicates, i.e. asbestos [35].

3.3. Phase transitions

Diblock and triblock semifluorinated n-alkanes exhibit solid–solid phase transitions observed by differential scanning calorimetric (DSC) measurements effected on some compounds of the $F_{12}H_m$ and $F_{12}H_mF_{12}$ series in order to gather information on their behaviour towards an increase in temperature [24,26,32]. DSC curves of diblock semifluorinated n-alkanes with $4 \leq m \leq 14$ generally show a strong melting endotherm, plus a broader, weaker endotherm (Fig. 8). This latter endotherm is generally associated with a solid–solid phase transition whose temperature, corresponding to the maximum in the endotherm, was found to increase with the hydrogenated segment length. For $F_{12}H_{14}$, the transition temperature is too close to the melting endotherm to allow quantitative analysis.

The observed melting temperatures also increase with the hydrogenated segment length and fall on at least three distinct curves (Fig. 9):

1. When $n=m$, the curve exhibits the largest slope, comparable with that of fluorocarbons ($m=0$).
2. For $F_{12}H_m$ compounds, melting points lie on two different curves according to whether m is higher or lower than 12 (that corresponds to an abscissa of 24 backbone atoms). In particular, for compounds having longer hydrogenated sequences ($m>14$) the melting point behaviour appears to parallel that of hydrocarbons (lower continuous curve in Fig. 9).
3. For triblock $F_{12}H_mF_{12}$ compounds, the melting points curve shows an increase in slope as m becames smaller; the curve also tends to intersect the fluorocarbon melting curve at an abscissa value of 24 backbone carbons ($m=0$).

The melting point curves of fluorocarbons and hydrocarbons reported for comparison represent the limiting behaviour of the melting points for diblock and triblock semifluorinated n-alkanes. In fact, as the number of methylene units increases, the melting point curve approaches that for a hydrocarbon; this means that the effect of the fluorinated end-groups becomes more and more negligible. Hence, at

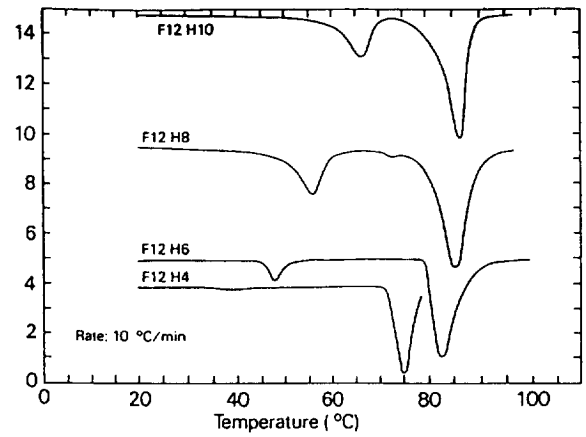

Fig. 8. DSC thermograms for some $F_{12}H_m$ compounds (taken from Ref. [32]).

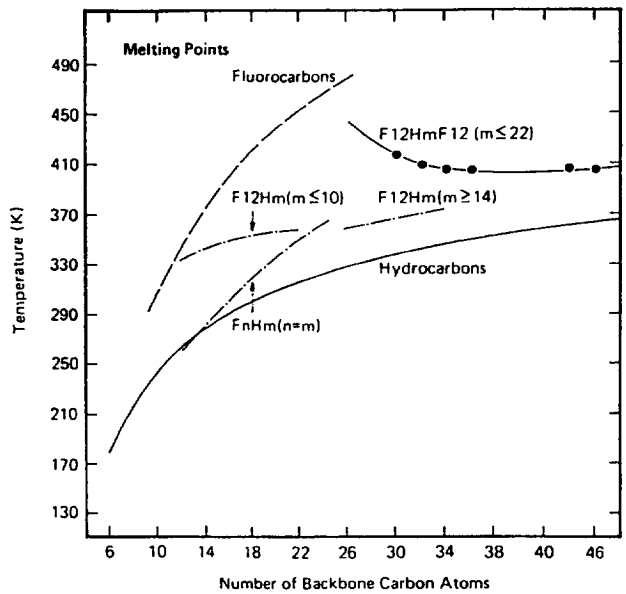

Fig. 9. Melting points determined for linear hydrocarbons, fluorocarbons, and F_mH_n (with $m=n$), $F_{12}H_m$ and $F_{12}H_mF_{12}$ compounds (taken from Ref. [24]).

Table 1
Temperatures (°C) and heats (J mol^{-1}) of the solid–solid transitions found for compounds of the series $F_{12}H_m$ and for triblock semifluorinated alkanes

m	$F_{12}H_m$				$F_{10}H_mF_{10}$		$F_{12}H_mF_{12}$	
	°C [a]	J mol^{-1} [a]	°C [b]	J mol^{-1} [b]	°C [b]	J mol^{-1} [b]	°C [b]	J mol^{-1} [b]
4	40	1.4	−126	0.7				
6	44	3.3	−109	0.5				
8	51	5.6	−81	2.4	−1	9.2		
10	66	7.5	−66	1.0			24	3.3
12	80	11.3	−57	1.8				

[a] Taken from Ref. [32].
[b] Taken from Ref. [26].

very large m values, the melting points should eventually coincide with those for hydrocarbons; on the other hand, as m becames creasingly small the melting point curve approaches that for the fluorocarbon.

This behaviour is indicative of the influence that the lengths of the fluorinated and hydrogenated segments have on the molecular structure of these semifluorinated compounds. In fact, depending upon the relative increase in n or m, the molecular structure approaches the fluorocarbon or hydrocarbon type, respectively.

Other information can be derived from measurements of the heat of fusion. The observed heats of fusion for diblock $F_{12}H_m$ semifluorinated alkanes exhibit rather unusual behaviour [31]. The initial value of 23.0 J mol^{-1} recorded for $F(CF_2)_{12}F$ ($m=0$) is depressed to a value of 20.8 J mol^{-1} for $m=2$; it gradually increases with the number of methylene units until a value of 26.0 J mol^{-1} is attained for $m=14$, but suddenly reaches values higher than 40 J mol^{-1} for $m \geq 16$. The initial relative insensivity of the heat of fusion to an increase in the number of methylene units suggests that the influence of the hydrogenated segment is negligible for $m \leq 14$; therefore, prior to melting, the molecular structure is similar to that found in the perfluorinated compounds. The considerable increase in the heat of fusion for $m \geq 16$ could reflect a fundamental change in the molecular packing due to the influence of the hydrogenated segment.

The heats of the solid–solid transition were also found to increase as m changed from 4 to 12. The recorded value changes from 1.4 J mol^{-1} for $m=4$ to 11.3 J mol^{-1} for $m=12$; for $F_{12}H_{14}$ the transition temperature was too close to the melting endotherm to provide useful information. In particular, extrapolation to $m=2$ yielded a value of 0 for the transition heat, which corresponds to the absence of a transition in $F_{12}H_2$ as observed. The increase in the transition heat was about 1 J mol^{-1} for each $-CH_2-$ unit added to the hydrogenated segment; this suggests that an increase in the methylene sequence does not have a great influence on even the solid–solid transition mechanism, at least for $m \leq 14$.

A second solid–solid phase transition was found at lower temperatures for diblock compounds of the series $F_{12}H_m$ with $4 \leq m \leq 14$ [26]. In Table 1, the heats of these transitions, reported together with the values measured for $F_{10}H_8F_{10}$ and $F_{12}H_{10}F_{12}$, are compared with those recorded at higher temperatures. As can be seen, the heats associated with the low-temperature solid–solid transition are much lower than those measured for the corresponding transitions at higher temperature.

Liquid–crystalline phase transitions were finally detected by light microscopy for $F_{10}H_{10}$ [33], $F_{10}H_{10}F_{10}$, $F_{12}H_8F_{12}$ and $F_{12}H_{12}F_{12}$ compounds [36]. In particular, $F_{10}H_{10}$ undergoes a reversible transition between two liquid–crystal phases both having a layered structure, while the other compounds reveal the formation, on heating the crystalline solid, of a smectic B phase, stable over a very narrow temperature range (0.4°C or less), before the isotropic phase was reached. The smectic B-isotropic transition occurred reversibly at the same temperature either on heating or on cooling. In particular, this temperature seems to be sensitive to the fluorinated segment length rather than that of the hydrogenated segment; in fact, it was 137.6°C for $F_{12}H_8F_{12}$ and 136.7°C for $F_{12}H_{12}F_{12}$, while a transition temperature of 111.8°C was determined for $F_{10}H_{10}F_{10}$.

4. Behaviour in solution

4.1. Surface activity

It is well known that fluorinated compounds have very low surface energies, so that many studies have been made. Semifluorinated n-alkanes can be considered as a new class of surfactant due to their behaviour in solutions of hydrocarbons or perfluoro compounds [37].

The mutual insolubility of hydrocarbons and fluorocarbons has been demonstrated for $C_{19}H_{40}/C_{20}F_{42}$ and $C_{20}H_{42}/C_{20}F_{42}$ binary systems, which show a phase separation in the liquid state by light microscopy [38]. The combination of alkane and perfluoroalkane segments on the same chain changes this situation. In fact, due to the presence of the unsymmetrical $-CF_2-CH_2-$ linkage they are more polar than either fluorocarbons or hydrocarbons; most are more soluble in polar solvents, e.g. methanol, than the analogous fluorocarbons or hydrocarbons. In particular, amphiphile-like behaviour was found when some diblock semifluorinated n-alkanes were

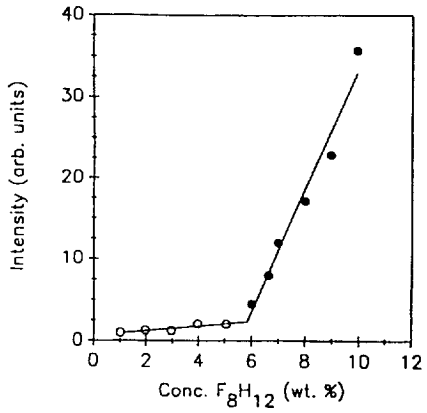

Fig. 10. Plot of Fluorescence intensity of 25-(NBD-methylamino)-27-norcholestryl oleate versus F_8H_{12} concentration (wt.%) in perfluorotributylamine (taken from Ref. [37]).

dissolved in either cyclic or linear hydrocarbons [39]. The formation of an isotropic liquid phase was observed for $F_8H_{12}/C_{20}H_{42}$ and $F_{12}H_8/C_{20}F_{42}$ binary sistems, being is favoured when a dominant group soluble in the second component was present; thus, in the $F_{12}H_8/C_{20}H_{42}$ binary system the isotropic liquid phase was not observed. A detergent behaviour can therefore be defined for diblock semifluorinated n-alkanes.

Some measurements of surface tension decrease have been performed in dodecane solutions of compounds of the series $F_{12}H_m$ [40], showing that the longer the hydrogenated chain length, the greater the surface tension depression. In contrast, with semifluorinated n-alkanes having the same hydrocarbon segment a longer fluorocarbon segment does not lead to a greater depression of the surface tension.

Evidence of reversed micelle formation in solutions of F_8H_{12} in perfluorotributylamine were also reported [37]. A steroid-based fluorescence probe has been used to establish a plot of fluorescence intensity versus the weight per cent concentration of the semifluorinated compound (Fig. 10). The qualitative form of this plot is typical of micellar solutions and a critical micellar concentration of 5.8% F_8H_{12} in perfluorotributylamine may be deduced. The suggested aggregation form is a reversed micelle in which the hydrogenated heads cluster to form a hydrocarbon core, whereas the perfluorinated tails remain at the outer layer of the aggregate.

4.2. 'Gel' phase formation

The formation of a new phase exhibiting gel-like characteristics was noted during investigations on binary mixtures of semifluorinated n-alkanes in hydrocarbons [39,41] or other solvents [42]. This phase was observed when a semifluorinated n-alkane mixed with a liquid hydrocarbon, e.g. octane, decane, dodecane or cyclodecane, or a solvent, e.g. ethanol, acetone or tetrahydrofuran, was heated to form a homogeneous liquid and then allowed to cool to room temperature. The transition between this opaque phase and the transparent liquid one is reversible; it occurs at a temperature which depends on the concentration of the semifluorinated compound in the mixture and can be detected as a broad endotherm by DSC measurements (Fig. 11).

Fig. 12 represents the phase diagram obtained by plotting the recorded endotherms versus the concentration. A positive curvature towards higher temperatures can be observed at intermediate concentrations, reflecting an intermolecular interaction between the semifluorinated compound and the solvent. This interaction is confirmed by the change in shape of the phase diagram which occurs in going from linear to cyclic hydrocarbons.

These results indicate that the structure of the gel phase is different from that of the solid state. A structure has been suggested consisting of tightly interlaced crystallites which enclose large amounts of solvent in the cavities formed during crystallization [26]. The crystal size and the number of crystallites per volume depend on the crystallization conditions. Thus, fast cooling gives multiple nucleation, while slow cooling results in a network with a smaller mesh size. The formation of these crystallites can be related to the bilayered lamellar structure of these semifluorinated molecules. Since gels are also formed in fluorocarbon solvents, one can suggest that the nucleation process starts with a regular packing of

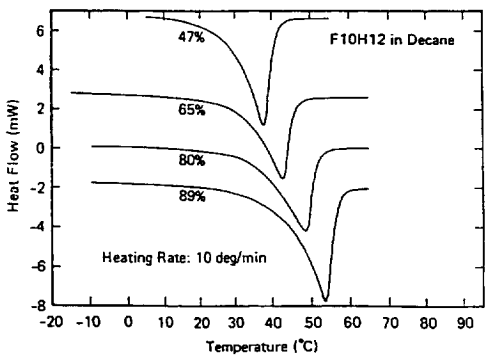

Fig. 11. DSC endotherms of $F_{10}H_{12}$ in decane at various concentrations (taken from Ref. [41]).

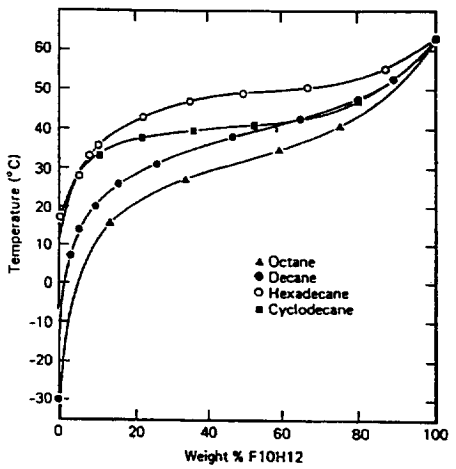

Fig. 12. Phase diagrams of $F_{10}H_{12}$ in various hydrocarbons (taken from Ref. [41]).

the fluorocarbon segments at all temperatures below the melting point. Crystal growth is fast in the direction parallel to the lamellar surface where aggregation of the perfluorinated segments in an ordered layer is possible, whereas in the direction normal to the lamellar surface such aggregation requires a slower deposition of the hydrogenated segments on a less regular surface. In this manner very long needles are formed in a disordered network; these needles can reach a length greater than 0.5 cm, while their thickness is less than few μm.

5. Chemical stability

Due to their characteristic structure, diblock and triblock semifluorinated n-alkanes maintain the typical chemical stability of perfluorocarbons and hydrocarbons. Nevertheless, the $-CF_2-CH_2-$ linkage at the junction point of the perfluorinated and the hydrogenated segments may insert an element of instability into the molecule. Some experiments carried out in an alkaline medium have indicated very low concentrations of F^- in the reaction mixture [43], thus confirming the stability of F_mH_m compounds. More recently, mass spectrometric studies on a series of diblock semifluorinated n-alkanes [44] have confirmed this stability and shown a low abundance of fragments corresponding to cleavage of the $-CF_2-CH_2-$ bond. Both positive-ion EI or negative-ion mass spectra suggest the presence of an F···H bridge between the zig-zag hydrogenated segment and the helical fluorinated one, thus conferring a particularly high strength on the $-CF_2-CH_2-$ bond.

6. Applications

The applications so far suggested for semifluorinated n-alkanes mainly fall within the biomedical field. Thus, some triblock semifluorinated n-alkanes, e.g. 1,2-(perfluorodialkyl)ethanes, have been proposed as potential oxygen-carrying agents for blood substitutes [45]. More recently, the same use has also been suggested for diblock semifluorinated n-alkanes [46–52]. Due to their very weak intermolecular forces, highly fluorinated liquids are in fact known to dissolve significant quantities of various gases such as oxygen, nitrogen, carbon dioxide, hydrogen and noble gases. In particular, NMR studies show that the structure of the fluid, rather than attractive oxygen–fluorine forces, seems to play a predominant part in oxygen solubility [53]. For non-associated liquids such as fluorocarbons and hydrocarbons, the structure depends principally on the molecular shape [54]. Thus, the presence of fluorine atoms which are larger than hydrogen atoms on a carbon chain makes a more irregular molecular shape, producing numerous large-sized cavities in the liquid. This can explain the lower boiling points and higher viscosity of these compounds [55], and their ability to dissolve significant amounts of gases.

This characteristic, together with their high chemical inertness and stability, has determined the choice of these compounds as the main component ensuring a gas-transporting function in blood substitute emulsions and in breathing liquids. However, because of their very poor solubility in water, perfluorinated compounds can be used for these applications only in an emulsion, which has to possess a definite intravascular stability depending on its colloidal properties and, above all, on the particle size. Emulsion systems are thermodynamically unstable and physical changes often occur over time. In particular, a molecular diffusion process can occur consisting of the coalescence of two or more bubbles into a single one. This process leads to the formation of bigger bubbles, with subsequent degradation of the emulsion.

In order to increase the emulsion stability, diblock semifluorinated compounds have been proposed as a third component having an interfacial activity [56]. Even at small concentrations, these stabilizing compounds completely cover the perfluorocarbon bubbles with a monomolecular film at the perfluorocarbon/water interface, thus hindering their coalescence. The effect of small amounts (1% w/v) of some diblock semifluorinated n-alkanes on the rate of growth of perfluorodecalin particles is demonstrated by the following data: the volume of a cube of bubbles of mean diameter after storage for 30 changes from about 14×10^{-21} m^3 for perfluorodecalin stabilized by Pluronic F68 (the most commonly used surfactant for perfluorocompound emulsification) to about 7, 6 and 4.5×10^{-21} m^3 in the presence of 1% w/v of F_6H_8, F_8H_2 and $F_{10}H_2$, respectively [56]. Accordingly, the curves of interfacial tension show a rapid initial decline and reach a plateau at concentrations below 2%; this suggests that, at the perfluorocarbon/water interface, the semifluorinated n-alkane has the perfluorinated segment on the inside and the hydrocarbon chain on the outside of the perfluorocarbon bubble. In this way, the hydrocarbon chain also acts as an anchor group for lipophilic surfactants, so contributing to the stabilization of the emulsion.

The use of some unsaturated diblock semifluorinated n-alkanes was also suggested in ophtalmology [29,57] in place of the already investigated, but too toxic, perfluorodecalin [58,59]; their use could also favour tissue cicatrization in vitreoretinian surgery.

Another recent application for semifluorinated n-alkanes is their use as additives in the ski-wax preparation [60]. In this case, the most important property of these compounds is their typical water-repellence, which is very important under moist snow conditions. In fact, for amounts of water of less than 1% the friction depends principally on the internal rolling of the snow crystals due to the ski shearing stress, while with larger amounts of water (moist snow) the water-repellence becomes the decisive factor.

7. Conclusions

Diblock and triblock semifluorinated n-alkanes can be considered as a class of compounds with particular characteristics

and properties. Investigations performed by different techniques, i.e. DSC, Raman spectroscopy, small angle X-ray scattering and light microscopy, have provided much information on the crystalline state of these compounds and on their behaviour on heating.

Thus, in the crystal lattice of diblock compounds at least three modes of molecular packing (*parallel*, *antiparallel* and *bilayered* packing) were found depending on the n/m ratio. Moreover, each molecule presents a planar zig-zag portion corresponding to the hydrogenated segment, isolated from the adjacent hydrocarbon chains and joined to a helical fluorinated portion. A new model proposed more recently suggests the formation of layers of cylindrical crystallites instead. A solid–solid phase transition occurs below the crystal melting point; above the melting point, only the hydrogenated portion of the molecule disorders while the fluorinated segment remains rigid. For some diblock and triblock semifluorinated compounds, liquid–crystalline phase transitions were also detected just before the isotropic liquid-phase formation.

Measurements of the surface tension of dilute solutions of some diblock semifluorinated compounds in hydrocarbons revealed a certain surface activity; these compounds also exhibit surfactant behaviour, so that they can be defined as a new class of surfactants. Moreover, for some the formation of a characteristic gel-like phase was observed when their solutions in an organic solvent were cooled.

Finally, the use of semifluorinated n-alkanes in the biomedical field as oxygen-carrying agents and as co-surfactants in microemulsions was recently suggested and is at present under experimental study.

Acknowledgements

The author wish to thank the editors and the authors who have permitted the reproduction of the figures in this article.

References

[1] R.N. Haszeldine, D.W. Keen and A.E. Tipping, *J. Chem. Soc. C*, (1970) 414.
[2] F. Jeanneaux, M. Le Blanc, A. Cambon and J. Guion, *J. Fluorine Chem., 4* (1974) 261.
[3] R. Gregory, R.N. Haszeldine and A.E. Tipping, *J. Chem. Soc. C*, (1971) 1216.
[4] N.O. Brace, *J. Org. Chem., 37* (1972) 2429.
[5] P. Calas, P. Moreau and A. Commeyras, *J. Chem. Soc., Chem. Commun.*, (1982) 433.
[6] R.N. Haszeldine and B.R. Steele, *J. Chem. Soc.*, (1953) 1199.
[7] G. van Dyke Tiers, *J. Org. Chem., 27* (1962) 2261.
[8] N.O. Brace, *J. Org. Chem., 28* (1963) 3093.
[9] D.J. Burton and L.J. Kehoe, *J. Org. Chem., 35* (1970) 1339.
[10] D.J. Burton and L.J. Kehoe, *J. Org. Chem., 36* (1971) 2596.
[11] Ph. Laurent, H. Blancou and A. Commeyras, *J. Fluorine Chem., 62* (1993) 173.
[12] Q.Y. Chen, Z.M. Qiu and Z.Y. Yang, *J. Fluorine Chem., 36* (1987) 149.
[13] Q.Y. Chen and M.F. Chen, *Chin. J. Chem. 9* (1991) 186.
[14] N.O. Brace, *J. Org. Chem., 27* (1962) 3027.
[15] N.O. Brace, *J. Org. Chem., 27* (1962) 3033, 4491.
[16] N.O. Brace, *J. Org. Chem., 31* (1966) 2879.
[17] N.O. Brace, US Pat. 3 145 222, 1964.
[18] N.O. Brace, *J. Org. Chem., 38* (1973) 3167.
[19] W. Dmowski, *J. Fluorine Chem., 50* (1990) 319.
[20] N.O. Brace, *J. Fluorine Chem., 20* (1982) 213.
[21] M. Napoli, C. Fraccaro, L. Conte, G.P. Gambaretto and E. Legnaro, *J. Fluorine Chem., 57* (1992) 219.
[22] A. Hassner, R.P. Hoblitt, C. Heatcock, J.E. Kropp and M. Lorber, *J. Am. Chem. Soc., 92* (1970) 1326.
[23] J.F. Rabolt, T.P. Russel and R.J. Twieg, *Macromolecules, 17* (1984) 2786.
[24] R.J. Twieg and J.F. Rabolt, *Macromolecules, 21* (1988) 1806.
[25] M.V.D. Puy, A.J. Poss, P.J. Persichini and L.A.S. Ellis, *J. Fluorine Chem., 67* (1994) 215.
[26] J. Höpken, C. Pugh, W. Richtering and M. Möller, *Makromol. Chem., 189* (1988) 911.
[27] P.L. Coe and N.E. Milner, *J. Organometal. Chem., 39* (1972) 395.
[28] B. Escoula, I. Rico, J.P. Laval and A. Lattes, *Synth. Commun., 15* (1985) 35.
[29] I. Rico-Lattes, B. Guidetti, V. Emmanouil and A. Lattes, *L'actual. Chim.*, (June–July 1995) 47.
[30] N.O. Brace, *J. Am. Chem. Soc., 86* (1964) 523.
[31] K. von Werner, Ger. Offen. DE 3 925 525, 1991; [*Chem. Abs., 114* (1991) 184 774 g].
[32] T.P. Russell, J.F. Rabolt, R.J. Twieg, R.L. Siemens and B.L. Farmer, *Macromolecules, 19* (1986) 1135.
[33] C. Viney, T.P. Russell, L.E. Depero and R.J. Twieg, *Mol. Cryst. Liq. Cryst., 168* (1989) 63.
[34] J. Höpken and M. Möller, *Macromolecules, 25* (1992) 2482.
[35] E.J.W. Whittaker, *Acta Crystallogr., 10* (1957) 149, and references cited therein.
[36] C. Viney, R.J. Twieg, B.R. Gordon and J.F. Rabolt, *Mol. Cryst. Liq. Cryst., 198* (1991) 285.
[37] M.P. Turberg and J.E. Brady, *J. Am. Chem. Soc., 110* (1988) 7797.
[38] D.L. Dorset, *Macromolecules, 23* (1990) 894.
[39] R.J. Twieg, T.P. Russell, R. Siemens and J.F. Rabolt, *Macromolecules, 18* (1985) 1361.
[40] G.L. Gaines, Jr., *Langmuir, 7* (1991) 3054.
[41] J.F. Rabolt, T.P. Russell, R. Siemens, R.J. Twieg and B. Farmer, *Polym. Prepr., 27* (1986) 223.
[42] M. Napoli, A. Scipioni, M. Carbini and C. Fraccaro, *Proc. 11th Eur. Symp. Fluorine Chem., Bled (Slovenia)*, 17–22 Sept., 1995, p. 211.
[43] M. Meinert and A. Knoblich, *J. Fluorine Chem., 58* (1992) 201.
[44] M. Napoli, L. Krotz, L. Conte, R. Seraglia and P. Traldi, *Rapid Commun. Mass Spectrom., 7* (1993) 1012.
[45] J.G. Riess and M. LeBlanc, *Angew. Chem., 90* (1978) 654.
[46] C. Cecutti, I. Rico, A. Lattes, A. Novelli, A. Rico, G. Marion, A. Graciaa and J. Lachaise, *Eur. J. Med. Chem., 24* (1989) 485.
[47] C. Cecutti, A. Novelli, I. Rico and A. Lattes, *J. Dispers. Sci. Technol., 11* (1990) 115.
[48] H. Meinert, R. Fackler, A. Knoblich, J. Mader, P. Reuter and W. Rohlke, *Biomater., Artif. Cells, Immobilization Biotechnol., 20* (1992) 95.
[49] H. Meinert, R. Fackler, A. Knoblich, J. Mader, P. Reuter and W. Rohlke, *Biomater., Artif. Cells, Immobilization Biotechnol., 20* (1992) 805.
[50] J.G. Riess and M. Postel, *Biomater., Artif. Cells, Immobilization Biotechnol., 20* (1992) 819.
[51] H. Meinert and A. Knoblich, *Biomater., Artif. Cells, Immobilization Biotechnol., 21* (1993) 583.
[52] H. Meinert, *Macromol. Symp., 82* (1994) 201.
[53] M.A. Hamza, G. Serratrice, M.J. Stébé and J.J. Delpuech, *J. Magn. Reson., 42* (1981) 227.
[54] D. Chandler, *Annu. Rev. Phys. Chem., 29* (1978) 441.

[55] E.P. Wesseler, R. Iltis and L.C. Clark, *J. Fluorine Chem., 9* (1977) 137.
[56] H. Meinert, R. Fackler, A. Knoblich, J. Mader, P. Reuter and W. Röhlke, *Biomater., Artist. Cells Immobilization Biotechnol., 20* (1992) 95.
[57] I. Rico-Lattes, B. Feurer, B. Guidetti and V. Payrou, *Fr. Pat. 9 402 480*, 1994.
[58] S. Chang, *Am. J. Ophthamol., 103* (1987), 38.
[59] A. Mathis, *Visions Internationales*, No. 19 (1991) 16.
[60] G. Albanesi, *Chim. Ind. (Milan), 77* (1995) 377.